Structural and selectivity of 18-crown-6 ligand in lanthanide–picrate complexes

Muhammad I. Saleh [a,*], Eny Kusrini [a], Hoong K. Fun [b], Bohari M. Yamin [c]

[a] School of Chemical Sciences, Universiti Sains Malaysia, 11800 Penang, Malaysia
[b] School of Physics, Universiti Sains Malaysia, 11800 Penang, Malaysia
[c] School of Chemical Sciences and Food Technology, University Kebangsaan Malaysia, 43600 Bangi, Selangor, Malaysia

ABSTRACT

The selectivity factor in the separation of lanthanide could be associated with the coordination behaviour. Thus, we observed the study in the solid phase to understand the coordination pattern of Ln(III) with the 18-crown-6 (18C6) ligand. Good selectivity of the rigid 18C6 ligand toward Ln(III) depends on gradually smaller their ionic radii of Ln(III) in the complexes formation in the presence of picrate anion (Pic$^-$), i.e. lanthanide contraction and steric effects as clearly shown in the series of $[Ln(Pic)_2(18C6)]^+(Pic)^-$ {Ln = La, Ce, Pr, Nd, Sm, Gd} and $[Ln(Pic)_3(OH_2)_3] \cdot 2(18C6) \cdot 4H_2O$ {Ln = Tb, Ho} complexes. The La–Gd complexes crystallized in an orthorhombic with space group Pbca, while the Ho complex crystallized in triclinic with space group $P\bar{1}$. The lighter lanthanides complexes [La–Sm] had a 10-coordination number from the 18C6 ligand and the two picrates, forming a bicapped square-antiprismatic geometry. Meanwhile, the middle lanthanide complex [Gd] had a nine-coordination number from the 18C6 ligand and the two picrates, forming a tricapped trigonal prismatic geometry. The heavier lanthanide [Ho] is rather unique, since Ho(III) coordinated with nine oxygen atoms from three picrates and three water molecules in the opposite direction whereas three 18C6 molecules surrounded in the inner coordination sphere, forming a trigonal tricapped prismatic geometry. The 18C6 ligand is effective in controlling the molecular geometry and coordination bonding of Ln–O and can use a crystal engineering approach. No dissociation of Ln–O bonds in solution was observed in NMR studies conducted at different temperatures. The photoluminescence spectrum of the Pr complex has typical 4f–4f emission transitions, i.e. $^3P_0 \rightarrow {}^3F_2$ (650 nm), $^1D_2 \rightarrow {}^3F_2$ (830 nm) and $^1D_2 \rightarrow {}^3F_4$ (950 nm).

1. Introduction

Designing solid crystal architecture by using principles of crystal engineering is a new, growing area of inorganic, coordination and supramolecular chemistry [1–3]. These designs may be used for the rational development of novel functional materials with predictable bulk structure [4]. The main aim of crystal engineering is the non-casual synthesis of crystal complexes with deliberate reciprocal arrangement of the molecules in the crystal. Such crystal have intra and intermolecular covalent interaction i.e. coordination bonding, and non-covalent interactions i.e. hydrogen bonding, π–π interactions and van der Waals interactions. However, the relatively high energy of the interaction and its ability to generate recurrent patterns of intermolecular interactions in ways that govern the relative orientation of molecules entering the crystal [5].

The strategy of supramolecular synthesis includes the coordination centers and the bitopic connectors such as ligand and anion [2]. These bitopic connectors may be a relatively flexible structure that is sensitive to the environment in the crystal. These approaches can be used to design molecular structure and stabilize

one of the possible geometric configurations of the molecules [4]. In addition, hydrogen bonding can produce supramolecular structure [6] such as rows or helices (simulating regular polymer chains), layers, sheets and networks and induce supramolecular polar ordering [7]. These features are potentially important in several fields of material sciences [5].

Molecular coordination complexes of Ln(III) have attracted considerable attention, due to their applications in analytical and material chemistry [8–10]. Ln(III) forms various complexes with a high coordination numbers, usually >6 and sometimes as high as 9–10, with small donor atoms, such as oxygen and nitrogen a coordination number 12 can be achieved [11–17]. The coordination sphere of a central metal ion depends on the interplay between the ionic radius and the ion charge [18]. Generally, large ions can form a complex with the high coordination number. The most common ligands contain several oxygen donor atoms, for example, nitrates, phosphates, sulfates, oxalates, carboxylates, alcohols, crown ethers, Schiff bases and water molecules [19,20].

Complexes of Ln(III) and crown ethers and their derivatives in the presence of picric acid (Pic) have been previously described. These complexes include the benzo-15-crown-5 [21,22] and 1,3-phenylenebis(formyloxyacetyl-4'-benzo-15-crown-5) [23]. The cyclic polyether 18C6 ligand that is thought to control

* Corresponding author. Tel.: +60 4 6533888x3108; fax: +60 4 656646.
E-mail address: midiris@usm.my (M.I. Saleh).

molecular structure has been reported in alkaline–18C6 complexes [24–27]. The structure of the [alkaline–18C6]$^+$ fragment with the largest size metal ion is relatively rigid and exists as a half-sandwich encapsulate [24,27], with the small metal ion situated out of the crown ligand plane [27–30]. This distortion results from a mismatch between the metal ion and the crown ether cavity sizes [26,27], a demand for the most efficient interaction of the metal ion with the counter anion, a demand for dense packing of the structural component [24] and the dissymmetry of the environment of the inner coordination sphere from the two axial sides [4].

The selectivity of crown ether for Ln(III) has been used when to separate the lanthanides followed by quantitative determination of La(III) from rare earth bearing mineral by liquid–liquid extraction with dibenzo-24-crown-8 as the complexing agent [31]. With this selectivity in the liquid phase, the study continued in the solid phase to understand the coordination pattern of Ln(III) with oxygen donor atoms of the 18C6 ligand. The 18-crown-6 ligand has cavity diameter of 2.6–3.2 Å [24] and which matches the ionic diameter of the lanthanides (ionic diameter between 1.73 and 2.06 Å) [31]. We think that the coordination behaviour will be able to explain the selectivity factor in the separation. The similarities and the differences in the formation of coordination bonding of lanthanide–picrate complexes in the 18C6 closed system will be the main discussion in this paper.

2. Experimental

2.1. Preparation of 18C6–(Ln–Pic) complexes

La$_2$O$_3$ and 18-crown-6 [C$_{12}$H$_{24}$O$_6$] was purchased from Fluka Chemika (Buchs, Switzerland), Pr$_6$O$_{11}$, Nd$_2$O$_3$, Sm$_2$O$_3$, Gd$_2$O$_3$, Tb$_4$O$_6$ from Sigma (St. Louis, USA), Ho$_2$O$_3$ from RDH (Steinheim, Germany), picric acid (Pic) [(NO$_2$)$_3$C$_6$H$_2$OH] from BDH (Poole, England). Ce(NO$_3$)$_3$.6H$_2$O was obtained from Johnson Matthey Electronics (New Jersey, USA). All chemicals and solvents were of analytical grade and were used without further purification.

Lanthanide picrates of [Ln(Pic)$_2$(OH$_2$)$_6$]$^+$(Pic)$^-$ · 6H$_2$O {Ln = La–Ho} were prepared as previously described [32], as were the cyclic complexes [33]. A mixture of [Ln(Pic)$_2$(OH$_2$)$_6$]$^+$(Pic)$^-$ · 6H$_2$O (0.220 g, 0.21 mmol) was mixed with 18C6 (0.264 g, 1 mmol) in 20 mL CH$_3$CN. The solution was heated in a water bath with continuous stirring for 10–15 min at 80–90 °C. The mixture was left to stand for one day and single crystals for La (96%); Ce (80%); Pr (96%); Nd (96%); Sm (94%); Gd (50%) and Ho (50%) suitable for X-ray diffraction determination were collected. However, the reactions of [Tb(Pic)$_2$(OH$_2$)$_6$]$^+$(Pic)$^-$ · 6H$_2$O with the 18C6 ligand in acetonitrile did not result in single crystal products.

2.2. Physical measurements

The percentages of carbon, hydrogen and nitrogen were performed on a Perkin–Elmer 2400II Elemental Analyzer. Conductivity measurements were carried out in dimethyl sulfoxide (DMSO) solution at 26.3 ± 0.91 °C using a Scan500 conductivity meter. IR spectra were recorded on a Perkin–Elmer FTIR 2000 spectrophotometer in KBr pellets in the 4000–400 cm^{-1} regions. ^{1}H and ^{13}C NMR spectra were measured on a Bruker 400 MHz and 300 MHz spectrometer, respectively, with tetramethylsilane (TMS) as internal standard. Thermogravimetric analysis was recorded on a Perkin–Elmer TGA-7 series thermal analyzer (under nitrogen atmosphere) with a heating rate at 20 °C/min.

Photoluminescence (PL) measurements were made at room temperature by using a Jobin Yvon HR800UV system, with the data collected and processed with Labspec Version 4 software source. A HeCd laser was used for excitation at 325 nm and the emission

spectra were scanned from 330 to 1000 nm. An incident laser (20 mW) was used as an excitation source. A microscope objective lens (UV40×) was used to focus the laser on the sample surface. The emitted light was dispersed by a double grating monochromator (0.8 m focal length) equipped with an 1800 grove/mm holographic plane grating. Signals were detected with a Peltier-cooled CCD4 array detector.

2.3. X-ray crystallography analyses

X-ray single crystal data collected by using a Bruker APEX area-detector diffractometer with a graphite monochromatic Mo Kα radiation at a detector distance of 5 cm and with APEX software [34]. The collected data were reduced by using SAINT program and the empirical absorption corrections were performed with the SADABS program [34]. The structures were solved by direct methods and refined by least-squares using the SHELXTL software package [35]. All non-hydrogen atoms were refined anisotropically. Hydrogen atoms were located from difference Fourier maps and were isotropically refined. The final refinements converged well. Data for publication were prepared by using SHELXTL [35] and PLATON [36]. The structures of complexes were solved by direct methods and refined using the full-matrix least-squares method on F$_2^{obs}$ as implemented by the SHELXTL program [35].

3. Results and discussion

3.1. Physical properties and spectral analysis

The complexes are air-stable in solid state, soluble in dimethyl sulfoxide; moderately soluble in acetone, acetonitrile, tetrahydrofuran, methanol, water and ethanol and insoluble in chloroform, toluene and carbon tetrachloride. The elemental analyses of all of the cyclic complexes are consistent with the molecular formula derived from the single crystal X-ray diffraction (Table 1).

The solubility of all the complexes in common solvents is low which has made it difficult to do studies in solution and has prevented the measurement of conductivity. The molar conductance of the complexes in DMSO solution (see Table 1) indicates that the La–Gd complexes can act as ionic compounds [37], implying that only two Pic$^-$ ions are in the coordination sphere and that third Pic$^-$ ion is a counter anion. The Tb and Ho complexes are non-electrolyte compounds.

The infrared spectra of the 18C6 ligand and its complexes show the common behaviour [33]. On the basis of the similarity of their IR spectra, the La–Gd complexes are thought to have similar structures. On the other hand, the Tb and Ho complexes are analogs. Generally, the v(C–C) and v(C–O) stretching of the 18C6 ligand at 1280 and 1107 cm^{-1} was shifted to a lower frequency in the complexes at 1268 and 1105 cm^{-1}, respectively. The strong absorption at 2892 cm^{-1} weaken in complexes and was shifted to a lower frequency, indicating that the v(C–H) stretching is affected by neighboring O$_{etheric}$ bonded to Ln(III). The new sharp peak appearing at 1650–1300 cm^{-1} region was assigned to the asymmetric and symmetric of v(N–O) observed in the complexes. This indicates that the presence of Pic$^-$ ions and coordination with an oxygen atom from ortho-nitro group occurred. The IR spectra of the complexes show the disappearance OH out-of-plane bending vibration of the free Pic molecule at 1151 cm^{-1} indicating that the OH groups take part in coordination and the hydrogen atoms are substituted by Ln(III) [33,38–42]. The sharp bands at 1555 and 1342 cm^{-1} of the free Pic molecule were split into two double peaks at 1578; 1537 and 1368; 1334 cm^{-1}, respectively [33]. This results indicates that the Pic$^-$ ions were coordinated with Ln(III) in a bidentate manner [33,39–49]. Additionally, the broad bands at 3412–3413 cm^{-1}

Table 1
Elemental analysis of the 18C6–(Ln–Pic) complexes

Complex	C%, found (Calc.)	H%, found (Calc.)	N%, found (Calc.)	Decomposition point (°C)	Molar conductivity (Ω^{-1} mol^{-1} cm^3)
La	33.29 (33.01)	2.52 (2.75)	11.68 (11.55)	293.0–304.5	150
Ce	33.33 (32.97)	2.48 (2.75)	11.62 (11.54)	285.0–298.5	115
Pr	33.45 (32.95)	2.59 (2.74)	11.29 (11.53)	288.5–294.8	94
Nd	32.61 (32.84)	2.80 (2.74)	11.21 (11.49)	289.0–294.0	319
Sm	32.29 (32.66)	2.64 (2.72)	11.23 (11.43)	271.5–294.9	195
Gd	32.72 (32.55)	2.26 (2.71)	11.10 (11.39)	284.4–298.8	123
Tb	35.44 (32.94)	4.41 (4.44)	7.51 (8.23)	92.9–210.0	44
Ho	34.28 (32.81)	3.70 (4.43)	8.13 (8.20)	108.3–232.3	48

indicate that water is present in the Tb and Ho complexes, confirming the elemental analysis and decomposition point.

3.2. Thermal analysis

The results of thermal analysis studies identify the presence of the cyclic 18C6 ligand and the Pic$^-$ ions. Only the thermogram of the La–Sm complexes was obtained because of the explosive behaviour of the Pic$^-$ ion due to the presence of nitro groups. These complexes have a decomposition pattern similar to that as reported for the other lanthanide–picrate complexes [39–42,49]. The first step indicates decomposition of 18C6 ligand, which occurs between 105 and 250 °C. There was a rapid decomposition at 300–350 °C consistent with the removal of the 18C6 ligand and three picrates with the total mass reduction of 91% (Calc. 85%), giving the final products as lanthanide oxides at 600 °C. However, the Sm complex was more stable than the other Ln(III) complexes because it began to decompose at 250 °C and rapid decomposition occurred at 310–325 °C (40%).

3.3. NMR studies

The ^{1}H NMR study on the complexes verified the insertion of Ln(III) in the 18C6 ligand. NMR spectra were taken of the free 18C6 ligand and its complexes in dimethyl sulfoxide-*d* (DMSO-d_6). The ^{1}H NMR spectrum of the Pic molecule [40] shows two singlet peaks at 8.593 and 4.577 ppm assigned to the equivalents of two protons from the aromatic ring and one proton from the phenolic group, respectively. The proton peak of the phenolic group in Pic disappeared in all of the complexes, indicating that Ln(III) replaced the hydrogen atom via deprotonization or substitution [40]. At 25 °C, the 18C6 ligand has only one singlet peak at 3.519 ppm assigned to etheric groups (24H) due to its symmetric nature. The protons of the etheric groups peak in the Pr, Nd and Gd complexes were shifted downfield by 0.001 ppm and for the Tb complex this peak was also shifted downfield by 0.024 ppm. The protons from the etheric groups in the La, Ce and Sm complexes were shifted upfield by 0.02–0.03 ppm relative to the chemical shift of the free 18C6 ligand. No shifts was observed in the Ho complex, indicating that Ho(III) did not coordinate with the 18C6 ligand. These data are consistent agreement with the X-ray diffraction data. It can be concluded that the presence of Ln(III) in the complexes enable the etheric proton's peak were shifted downfield, due to the electronic effect between the 18C6 ligand and Ln(III), thus the electron density around the etheric proton decreased and deshielding.

The dynamic properties and reversible behaviour of the complexes were also undertaken by using ^{1}H NMR spectrometer at increasing temperature from 25 to 100 °C as shown in Fig. 1a and b. Similar ^{1}H NMR spectra were obtained when the temperature was reduced from 100 to 25 °C. The proton of the etheric group peaks was a consistent singlet peak regardless of increasing temperature and shifted downfield that indicating the coordina-
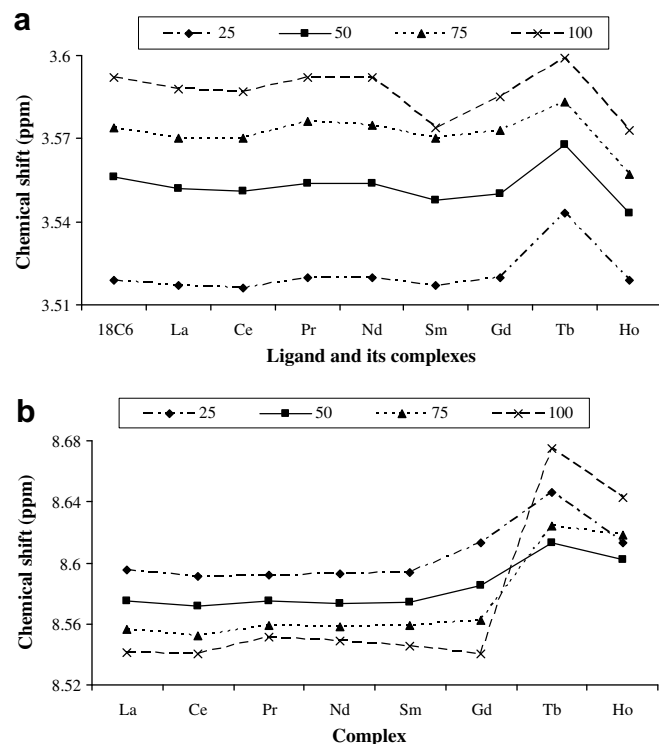
Fig. 1. Chemical shift of the free 18C6 ligand and its complexes at increasing temperature from 25 to 100 °C for the etheric proton of the 18C6 ligand (a) and protons from the aromatic rings of Pic$^-$ anion (b).

tion bond of Ln–O$_{18C6}$ is stronger than what was found at room temperature. Decreasing of temperature was implemented in all of the complexes had similar spectra, indicating that the reversible behaviour may be due to no dissociation of Ln–O bonds in the complexes.

3.4. X-ray studies

We structurally characterized new lanthanide–picrate complexes with the 18C6 ligand to form complexes with molecular formula of [Ln(Pic)$_2$(18C6)]$^+$(Pic)$^-$ {Ln = La, Ce, Pr, Nd, Sm and Gd} and [Ho(Pic)$_3$(OH$_2$)$_3$] · 2(18C6) · 4H$_2$O have been presented (Table 2). The La–Gd complexes crystallized in an orthorhombic with space group Pbca. From La to Ho, the ionic radii became gradually smaller. Therefore, the coordinated atoms around the different lanthanide ions are selective in number and type. Gd is located in the middle of the lanthanide series. The central Ln(III) has 10-coordinates with six oxygen atoms from the 18C6 ligand, four oxygen atoms from the two picrates, which are opposite one another with in the inner coordination sphere and almost perpendicular to each

Table 2
Crystallography data and their refinement of the 18C6–(Ln–Pic) complexes

Parameter	Complex			
	La	Ce	Pr	Nd
Formula	$C_{30}H_{30}N_9O_{27}La$	$C_{30}H_{30}N_9O_{27}Ce$	$C_{30}H_{30}N_9O_{27}Pr$	$C_{30}H_{30}N_9O_{27}Nd$
Molecular weight	1086.91	1088.12	1089.54	1092.24
T (K)	293	293	293	293
Crystal system	Orthorhombic	Orthorhombic	Orthorhombic	Orthorhombic
Space group	$Pbca$	$Pbca$	$Pbca$	$Pbca$
Unit cell dimensions				
a (Å)	11.122(6)	11.138(3)	11.122(2)	11.068(2)
b (Å)	23.870(12)	23.794(5)	23.722(4)	23.607(3)
c (Å)	30.051(15)	30.049(7)	30.011(5)	29.873(4)
$\alpha = \beta = \gamma$ (°)	90	90	90	90
Volume (Å^3)	7978.0(7)	7964.0(3)	7918.0(2)	7805.0(2)
Z	8	8	8	8
D_{calc} (g/cm^3)	1.185	1.257	1.346	1.447
Absorption coefficient (mm^{-1})	1.811	1.816	1.828	1.860
$F(000)$	4386	4376	4384	4392
Crystal size (mm)	0.15 × 0.25 × 0.44	0.08 × 0.43 × 0.50	0.15 × 0.25 × 0.44	0.31 × 0.32 × 0.49
θ Range (°)	1.36–27.00	1.70–27.50	1.36–27.00	1.36–27.60
h, k, l	−12/14, −30/26, −38/38	−13/14, −30/29, −29/38	−13/14, −29/30, −32/38	−13/14, −30/27, −38/38
Reflections collected/unique [R_{int}]	38650/8509 [0.056]	44863/9094 [0.042]	43753/8647 [0.043]	72019/9022 [0.031]
Data/restraint/parameter	8509/1/632	9094/0/641	8647/0/614	9022/0/604
Goodness-of-fit on F^2	1.043	1.164	1.032	1.069
Final R indices [$I > 2\sigma(I)$]	$R_1 = 0.048$, $wR_2 = 0.142$	$R_1 = 0.047$, $wR_2 = 0.092$	$R_1 = 0.037$, $wR_2 = 0.072$	$R_1 = 0.033$, $wR_2 = 0.086$
R indices (all data)	$R_1 = 0.080$, $wR_2 = 0.178$	$R_1 = 0.062$, $wR_2 = 0.098$	$R_1 = 0.060$, $wR_2 = 0.080$	$R_1 = 0.040$, $wR_2 = 0.090$

Parameter	Complex		
	Sm	Gd	Ho
Formula	$C_{30}H_{30}N_9O_{27}Sm$	$C_{30}H_{30}N_9O_{27}Gd$	$C_{42}H_{68}N_9O_{40}Ho$
Molecular weight	1098.98	1105.88	1503.98
T (K)	100	100	100
Crystal system	Orthorhombic	Orthorhombic	Triclinic
Space group	$Pbca$	$Pbca$	$P\bar{1}$
Unit cell dimensions			
a (Å)	10.976(2)	10.883(1)	13.894(3)
b (Å)	23.512(3)	23.360(3)	13.929(3)
c (Å)	29.683(4)	30.046(4)	17.362(3)
α (°)	90	90	75.979(1)
β (°)	90	90	70.844(1)
γ (°)	90	90	81.620(1)
Volume (Å^3)	7660.2(2)	7638.6(2)	3071.2(1)
Z	8	8	2
D_{calc} (g/cm^3)	1.652	1.856	1.400
Absorption coefficient (mm^{-1})	1.906	1.923	1.626
$F(000)$	4408	4424	1540
Crystal size (mm)	0.05 × 0.26 × 0.34	0.21 × 0.34 × 0.50	0.22 × 0.50 × 0.50
θ Range (°)	1.37–38.01	1.36–41.04	1.27–35.00
h, k, l	−18/18, −40/40, −51/51	−20/19, −43/43, −55/52	−22/22, −22/22, −28/28
Reflections collected/unique [R_{int}]	171986/20804 [0.050]	422992/25145 [0.051]	103345/26883 [0.027]
Data/restraint/parameter	20804/0/604	25145/0/605	26883/2/841
Goodness-of-fit on F^2	1.035	1.075	1.074
Final R indices [$I > 2\sigma(I)$]	$R_1 = 0.033$, $wR_2 = 0.064$	$R_1 = 0.031$, $wR_2 = 0.075$	$R_1 = 0.037$, $wR_2 = 0.099$
R indices (all data)	$R_1 = 0.055$, $wR_2 = 0.070$	$R_1 = 0.043$, $wR_2 = 0.082$	$R_1 = 0.042$, $wR_2 = 0.106$

other with dihedral angles of 84.0(3)–84.4(7)° for the La–Sm complexes (Fig. 2a). Outside the coordination sphere, there one picrate anion is a counter anion. Molecular structures of the La–Sm complexes are isostructural with the Eu complex [33].

The Gd complex has the same inner coordination sphere and similar outer coordination sphere with the La–Sm complexes except the nine-coordination number in the Gd complex. The Gd(III) ion is coordinated to the nine oxygen atoms from the 18C6 ligand in a hexadentate manner and the two picrates in each bidentate and monodentate manners through the phenolic oxygen and an oxygen of the *ortho*-nitro group in the opposite direction (Fig. 2b). The aromatic part of the coordinated picrates formed a dihedral angle of 82.7(6)°.

Unlike the La–Gd complexes, the Ho complex crystallized in a triclinic system with space group $P\bar{1}$ (Table 2). The Ho complex has centrosymmetrically two 18C6 molecules and non-centrosym-

metrically one 18C6 molecule surrounding the inner coordination sphere of [Ho(Pic)$_3$(OH$_2$)$_3$] due to a steric effect from three coordinated Pic$^-$ ions (Fig. 2c). The central Ho(III) ion in Fig. 2c is nine coordinated with six oxygen atoms from three Pic$^-$ ions and three oxygen atoms from three water molecules. Outside the coordination sphere, there are four water and three 18C6 molecules involved in structure act as solvated molecules. The Ho(III) ion has the smallest radius of the La–Gd ions, which requires smaller ligands and relatively fewer coordinated atoms around it because of the steric effects.

These clearly shows the lanthanide contraction effect because the Ln(III) coordination centers have large ionic radii, which influence the coordination number at the central atom and the geometry of the complex. Good selectivity of the rigid 18C6 ligand toward Ln(III) in the presence of Pic$^-$ ion which depends on the lanthanide contraction and steric effects were observed (Fig. 3a and b). The
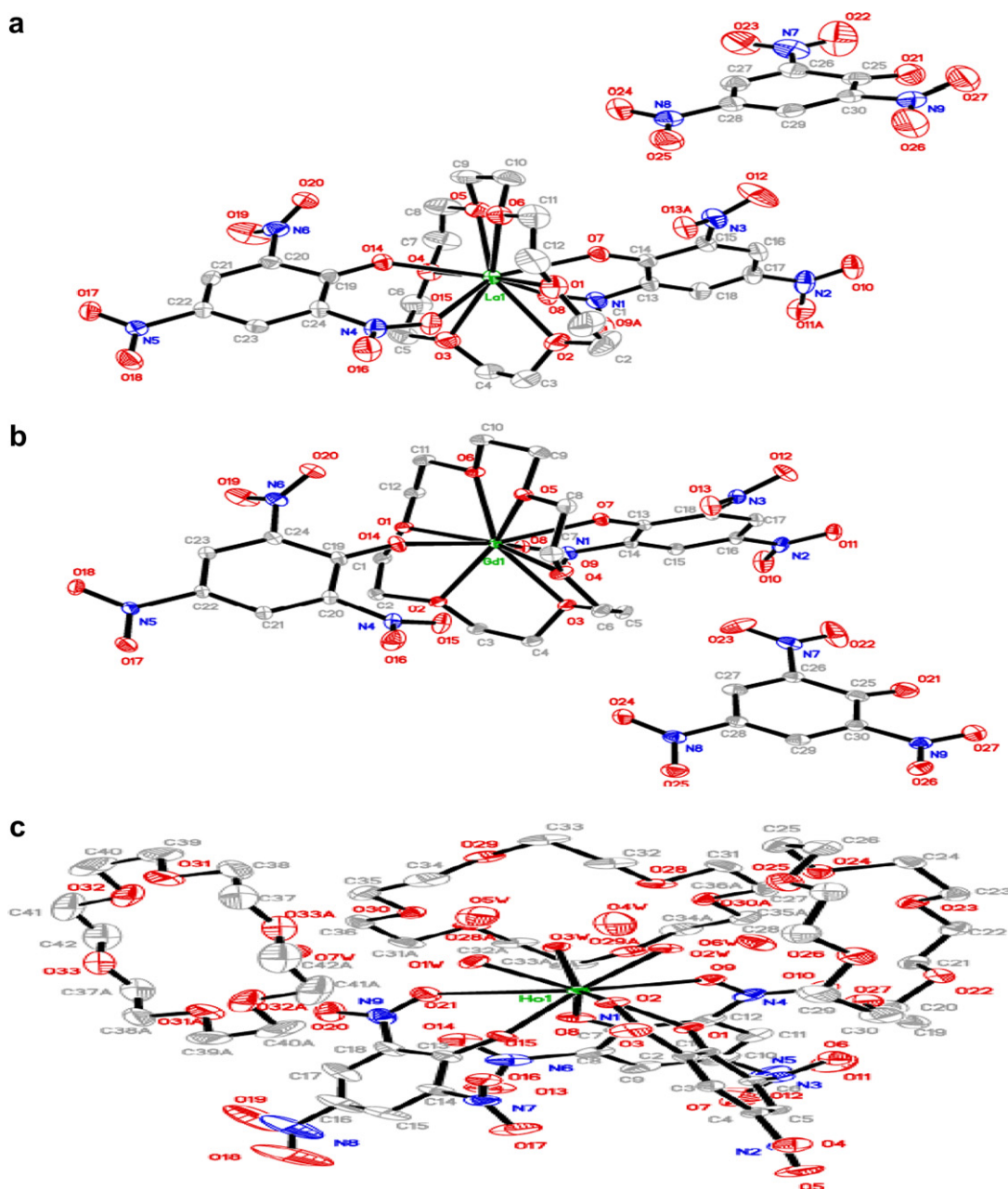
Fig. 2. Molecular structures of the La (a), Gd (b) and Ho (c) complexes with atom numbering scheme at the 50% probability level. All the hydrogen atoms were omitted for clarity.

a

[Ln(Pic)$_2$(OH$_2$)$_6$]$^+$[Pic]$^-$.6H$_2$O

Acetonitrile | Heat

[Ln(Pic)$_2$]$^+$ + mH$_2$O + [Pic]$^-$

Added

18C6

Heat

Slow evaporation

After one day

[Ln(Pic)$_2$(18C6)]$^+$[Pic]$^-$ + Solvent

Noted : for Ln = La - Gd

b

[Ln(Pic)$_2$(OH$_2$)$_6$]$^+$[Pic]$^-$.6H$_2$O

Acetonitrile | Heat

[Ln(Pic)$_2$(OH$_2$)$_3$]$^+$+ m H$_2$O + [Pic]$^-$

Added

18C6

Heat

Slow evaporation

After one day

[Ln(Pic)$_3$(OH$_2$)$_3$].2.(18C6).4H$_2$O + Solvent

Noted: for Ln = Tb and Ho
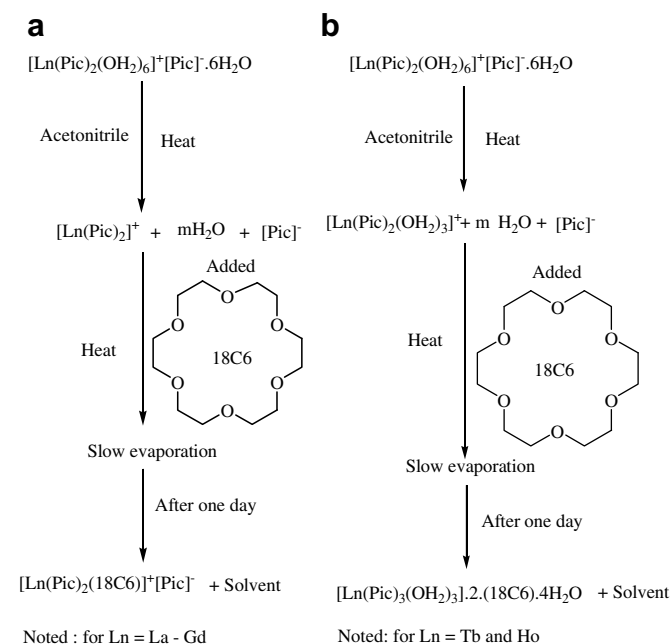
Fig. 3. Mechanism of reaction between lanthanide–picrate and the 18C6 ligand in acetonitrile for the La–Gd complexes (a) and the Tb and Ho complexes (b).

ionic radius of La(III), which is greater than the ionic radius of Gd(III), enabled interaction with more oxygen donor atoms to form a 10-coordinated complex while the smaller Gd(III) forms only a nine-coordinated complex. The steady decrease in Ln(III) radius can result in structural changes, with complexes of the early Ln(III) having higher coordination numbers than do the heavier lanthanide elements. The electronegativity also decreases as the lanthanide coordination number increases, and increases with the lanthanide atomic number. The Ln–O bond length decreases as the lanthanide atomic number increases and increases as the lanthanide coordination number increases. The hard polyether Lewis base crown ether saturates the coordination sphere and increases the coordination number, competing with complex formation reaction and the hydration side process to ultimately reach steric saturation around the Ln(III) central metal ion [18]. Thus, it is clearly observed that the small differences in the ionic radii play an important role in the selection of electron rich atoms for the formation of coordination bond.

The significant observations for the entire lanthanide series can be seen in the three representative structures that clearly indicate the changes in the 18C6 ligand to accommodate the decreasing sizes of the ionic radii (Fig. 2a–c). The La(III) ion has the largest effective ionic radius of 1.27 Å for a 10-coordination number [50], thus the 18C6 ligand could formed complexes without distorting as much as in complexes with the smaller Ln(III) ions. The La1 atom is coplanar with the O1, O3, O4 and O5 atoms and deviates by −1.218(4) Å for O2 atom and 0.991(4) Å for O6 atom from the ring 18C6 ligand in inner coordination sphere. For the Ce–Gd complexes, the Ln(III) ions in the ring 18C6 ligand of inner coordination spheres are only coplanar with three oxygen ether atoms of the 18C6 ligand and the other oxygen ether atoms of the 18C6 ligand are not coplanar. For the Ce complex, the Ce1 atom is coplanar with the O1, O5 and O6 atoms and displaces by −1.252(3) Å for O2 atom, 0.155(2) Å for O3 atom and 1.011(2) Å for O4 atom. For the Pr complex, the Pr1 atom is also coplanar with the O1, O2 and O6 atom and deviates by 1.029(2) Å for O3 atom, 0.174(2) Å for O4 atom and −1.276(3) Å for O5 atom. For the Nd complex, the Nd1 atom is coplanar with the O2, O3 and O4 atoms

and displaces by 1.030(3) Å for O1 atom, −1.291(3) Å for O5 atom and 0.188(3) Å for O6 atom. For the Sm complex, the Sm1 atom is also only coplanar with the O1, O2 and O6 atoms and deviates by 1.055(1) Å for O3 atom, 0.256(1) Å for O4 atom and −1.383(1) Å for O5 atom. For the Gd complex, the Gd1 atom is also coplanar with the O1, O2 and O6 atoms and displaces by −1.330(1) Å for O3 atom, 0.596(1) Å for O4 atom and 1.101(1) Å for O5 atom.

Water molecules may coordinate to the Ln(III) ions with small ionic radii e.g. Tb and Ho. These coordination results from the favorable matching between small ionic radii of Tb(III) and Ho(III) ions and the coordination binding, sometimes too long to be coordinated as an inner sphere ligand. Thus, the outer sphere of the complexes is obtained and the necessary coordination number is attained with three water molecules. The lack of saturation of
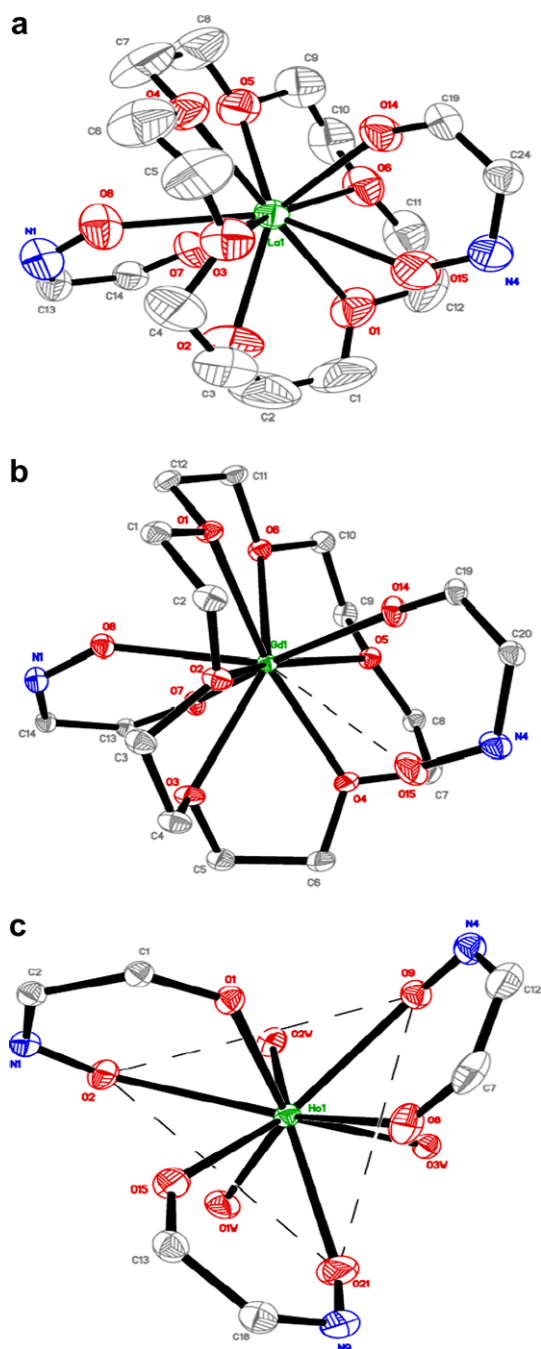
Fig. 4. The inner coordination spheres of [La(Pic)$_2$(18C6)]$^+$ (a), [Gd(Pic)$_2$(18C6)]$^+$ (b) and [Ho(Pic)$_3$(OH$_2$)$_3$] (c).
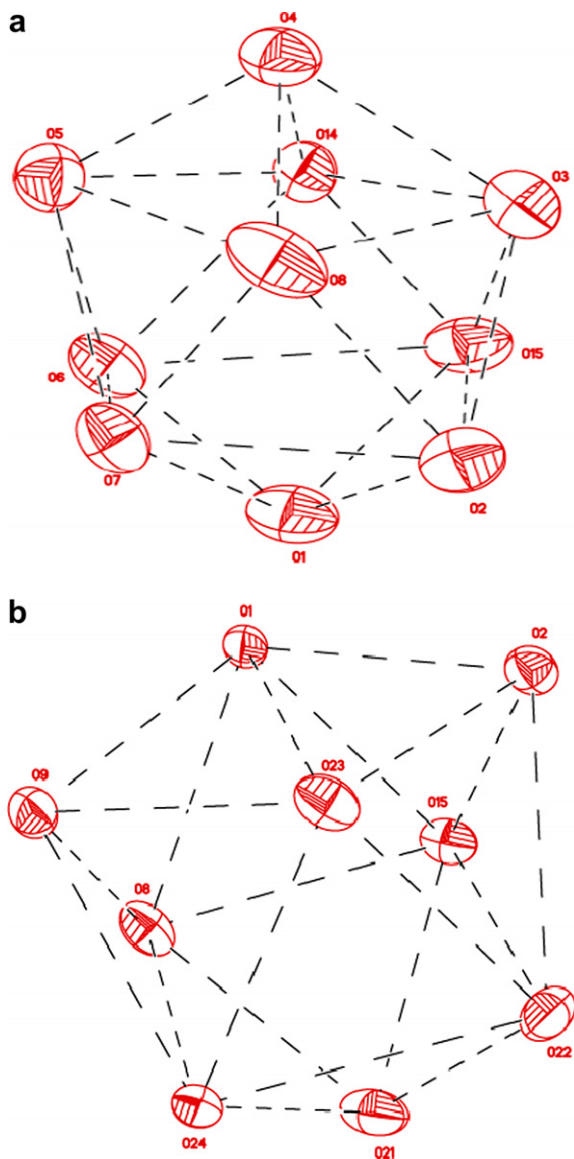
Fig. 5. Bicapped square antiprismatic geometry around La(III) (a) and tricapped trigonal prismatic geometry around Ho(III) (b).

the inner coordination sphere enables easy reactions either with a donor solvent or with a nucleophilic impurity such as water that ultimately leads to a poorly volatile or involatile hydroxo-complex.

All of the complexes we observed were mononuclear and the 18C6 ligand coordinated with Ln(III) in the hexadentate mode (for the La–Gd complexes). This pattern may be due to the presence of a second large ligand, i.e. the picrate anion, which coordinates with Ln(III) in a bidentate or monodentate chelating mode, making it difficult to form a polymer or a dimer. There is an uncoordinating picrate anion in the lattice as a counter anion in the La–Gd complexes. From our studies, the picrate anion is also significantly contributed to change of the geometries and formation of the complexes. Because of the picrate anion has higher steric hindrance to control the inner coordination sphere of the complexes than those found in the 18C6–Ln–Cl and 18C6–Ln–NO$_3$ complexes [51–55]. For the [LnCl(OH$_2$)$_2$(18C6)]Cl$_2$ · 2H$_2$O complexes {Ln = Pr–Tb} are isostructural with a nine-coordination number [51–53]. These similarities structures of the complexes did not show difference of ionic radii of the Ln(III) central ions. The chloride and nitrate anions have smaller steric hindrance than that found in the

picrate anion. Thus, the chloride and nitrate anion did not control and give an effect the inner coordination sphere of their complexes alike the picrate anion.

The inner coordination sphere of [Ln(Pic)$_2$(18C6)]$^+$ contains unequal bond lengths and forms a bicapped square antiprismatic geometry with the O1 and O4 atoms as the peak in the capping position (Fig. 4a). This geometry is slightly distorted due to the bond angle of two etheric oxygen atoms at the top in the capping position that is close to 180° (Fig. 5a). Gd(III) has a slightly distorted tricapped trigonal prismatic geometry with the O1, O3 and O5 atoms as the peaks in the capping position (Fig. 4b). The inner coordination sphere of [Ho(Pic)$_3$(OH$_2$)$_3$] has a trigonal tricapped prismatic geometry with the O2, O9 and O21 atoms coplanar and at the top in the capping position (Figs. 4c and 5b). The Ho1 atom lies on the base of the triangle (Fig. 4c).

The volume of the orthorhombic complexes generally decreases with increasing atomic number due to lanthanide contraction (Table 2). From the La–Gd complexes, the bond lengths between the Ln(III) ions and the coordinated atom from the same ligand tend to become shorter. The average bond length in the La–Gd complexes is 2.596(4), 2.584(3), 2.571(2), 2.550(2), 2.545(1) and 2.506(1) Å for Ln–O$_{18C6}$ bonds, respectively, indicating the effect of lanthanide contraction on molecular structure. These bond lengths were similar with those found in the 18C6–Ln–Cl complexes [51–53] and were shorter than what was found in the 18C6–Ln–NO$_3$ complexes [54,55]. The Ln–O15 bond length for one of the coordinated oxygen-nitro groups in the range 2.734(4)–2.789(1) Å was elongated by 0.055 Å in the La–Sm complexes (Table 3). In the Eu complex has the same inner coordination sphere and similar outer coordination sphere with the Gd complex except that the nine-coordination number for Gd issued [33]. The Eu–O15 bond length is 2.934(7) Å [33], while the non-bonding Gd–O15 bond length is 3.364 Å with an elongation distance of 0.43 Å (Fig. 4b).

The [Ln(Pic)$_2$(18C6)]$^+$(Pic)$^-$ complexes have an average C–O bond length of 1.427(8)–1.442(2) Å, but the average C–C bond length of 1.432(1)–1.499(2) Å. The coordination of Ln–O$_{18C6}$ in the inner coordination sphere is very much affected by the bond length and with the C–O bond length increasing while the C–C bond length decreasing. The O–Ln–O bond angles in all of the [Ln(Pic)$_2$(18C6)]$^+$(Pic)$^-$ complexes are equivalent (slightly bigger than 60°) (Table 4). The average C–O–C bond angle decreases with the size of the Ln(III) ions, namely 115.0(6)–112.6(1)° for the La–Gd complexes. The average O–C–C bond angle also decrease with the increase in the atomic number of lanthanides for the La–Gd complexes, namely 110.7(6)–107.0(1)°.

The O–C–C–O torsion angle [average of 49.2(6)–54.3(2)°] for the [Ln(Pic)$_2$(18C6)]$^+$(Pic)$^-$ complexes occur different conformational patterns in the respective order g$^-$g$^-$g$^-$g$^+$g$^-$g$^+$; g$^+$g$^-$g$^+$g$^-$g$^+$g$^-$g$^+$; g$^-$g$^+$g$^-$g$^+$g$^+$g$^+$; g$^+$g$^-$g$^+$g$^+$g$^+$g$^-$; g$^+$g$^-$g$^+$g$^-$g$^-$g$^-$ and g$^+$g$^-$g$^-$g$^-$g$^+$g$^-$ for the La–Gd complexes (Table 4). The average C–O–C–C torsion angle in ranges from 145.4(7)–158.9(5)° and was observed in the La–Gd complexes. The average O–C–C–O torsion angle of the solvated 18C6 A with g$^+$g$^-$g$^+$g$^-$g$^+$g$^-$ pattern [77.3(3)°], centrosymmetry B with g$^+$g$^+$ pattern [61.5(4)°] and centrosymmetry C with g$^+$g$^-$g$^+$ patterns [176.6(3)°] and observed in the Ho complex. The average C–O–C–C torsion angle of the solvated 18C6 for A, B and C fragments are 158.5(2), 140.7(2) and 176.6(3)°, respectively.

The crystal packing of the complexes shows the intra- and intermolecular C–H···O hydrogen bonding with one-dimensional (1-D) networks for the La–Gd complexes (Fig. 6a). Hydrogen bonding which is a non-covalent bond interaction will facilitate the formation of supramolecular architecture. Because of the different inner coordination spheres and outer spheres, the La–Gd and Ho complexes have different crystal structures. Their supramolecular architectures are built in different ways.

Table 3
Selected bond length (Å) in the 18C6–(Ln–Pic) complexes

Bond	Complex						
	Length (Å)						
	La	Ce	Pr	Nd	Sm	Gd	Ho
Ln1–O1	2.586(4)	2.549(3)	2.623(2)	2.513(2)	2.614(1)	2.580(1)	–
Ln1–O2	2.614(4)	2.551(3)	2.531(3)	2.510(2)	2.504(1)	2.508(1)	–
Ln1–O3	2.604(4)	2.570(3)	2.536(2)	2.606(2)	2.489(1)	2.567(1)	–
Ln1–O4	2.647(4)	2.601(3)	2.555(2)	2.565(2)	2.520(1)	2.448(1)	–
Ln1–O5	2.560(4)	2.602(3)	2.592(3)	2.574(2)	2.584(1)	2.462(1)	–
Ln1–O6	2.567(4)	2.633(3)	2.586(2)	2.533(2)	2.557(1)	2.471(1)	–
Ln1–O14	2.419(4)	2.410(2)	2.390(2)	2.341(2)	2.312(1)	2.263(1)	2.284(2)
Ln1–O7	2.449(3)	2.382(3)	2.356(2)	2.374(2)	2.354(1)	2.331(1)	2.290(2)
Ln1–O1	–	–	–	–	–	–	2.285(1)
Ln1–O8	2.637(4)	2.738(3)	2.749(3)	2.576(2)	2.521(1)	2.474(1)	2.571(2)
Ln1–O15	2.734(4)	2.624(3)	2.604(3)	2.744(3)	2.789(1)	–	2.582(2)
Ln1–O21	–	–	–	–	–	–	2.562(2)
Ln1–O1W	–	–	–	–	–	–	2.305(2)
Ln1–O2W	–	–	–	–	–	–	2.326(2)
Ln1–O3W	–	–	–	–	–	–	2.321(1)

Table 4
Selected bond angle and torsion angle (°) in the 18C6–(Ln–Pic) complexes

Bond	Complex					
	Angle (°)					
	La	Ce	Pr	Nd	Sm	Gd
O1–Ln1–O2	61.8(1)	64.0(1)	62.0(8)	64.4(7)	62.4(3)	64.0(3)
O2–Ln1–O3	62.5(1)	61.8(1)	64.4(9)	62.0(7)	65.3(3)	63.6(3)
O3–Ln1–O4	62.2(1)	62.1(1)	61.8(9)	62.4(7)	62.1(4)	63.0(3)
O4–Ln1–O5	61.7(1)	62.8(1)	62.2(9)	63.0(8)	62.9(4)	63.3(3)
O5–Ln1–O6	63.9(1)	62.2(9)	62.9(8)	62.4(8)	63.5(4)	65.3(3)
O6–Ln1–O1	61.8(1)	61.9(9)	62.4(8)	62.0(8)	63.0(3)	62.9(3)
Bond	Torsion angle (°)					
O1–C1–C2–O2	−41.2(12)	−55.6(5)	−48.7(5)	55.0(4)	53.8(2)	−55.2(1)
O2–C3–C4–O3	−56.4(7)	50.7(5)	54.7(5)	−49.2(5)	−55.3(2)	−57.2(2)
O3–C5–C6–O4	−48.8(9)	−43.8(8)	−50.4(5)	52.2(4)	50.3(2)	−48.7(2)
O4–C7–C8–O5	46.8(10)	47.5(5)	45.4(6)	56.9(4)	−52.5(2)	51.0(1)
O5–C9–C10–O6	−55.8(8)	−50.0(6)	56.9(4)	47.6(5)	−58.7(2)	−52.6(1)
O6–C11–C12–O1	50.6(8)	47.9(7)	51.1(5)	−50.5(4)	−55.1(2)	51.9(2)

The intermolecular O–H···O hydrogen bonding between the lattice water and the coordinating water or between the lattice water molecules form an infinite, one-dimensional (1-D) network with symmetry direction [010] and was observed only in the crystal packing of the Ho complex (Fig. 6b). One weak intramolecular C23–H23B···O22 [2.589 Å] hydrogen bond also was observed (Table 5). The van der Walls interactions of C19–H19A···Cg1 [3.009 Å] and C39–H39B···Cg3 [2.979 Å] with symmetry codes *x*, *y*, *z* and 1 − *x*, 1 − *y*, 1 − *z*, respectively, was observed only in the Ho complex where Cg1 = aromatic ring of (C1–C6) and Cg3 = aromatic ring of (C13–C18). A long contact of O···O and O···N also contributed to the strength of the hydrogen bonding.

3.5. Photoluminescence (PL) studies

The ability of the cyclic 18C6 ligand to satisfy the coordination requirements of Ln(III) centre with a high coordination number is an important criterion in the design of supramolecular photonic devices. The PL spectra of the free 18C6 ligand and its complexes were obtained when excited by absorption at 325 nm. The lowest triplet state energy level (T_1) of the 18C6 ligand which was calculated from the phosphorescence spectrum of the Gd complex indicates that the $T_1(L)$ of 18 762 cm^{-1} matches the resonance level of Sm(III) ion. This energy level is above the lowest excited resonance level $^4G_{5/2}$ (17 900 cm^{-1}) of Sm(III) and $^3S_2$ (18 182 cm^{-1}) of Ho(III) ions. How-

ever, the $T_1(L)$ is below of the lowest excited resonance level $^5D_4$ (about 20 400 cm^{-1}) of Tb(III) ion, not matched with the lowest excited level of Tb(III). Thus, the intramolecular energy transfer from the 18C6 ligand to Tb(III) is probably not occurred. To improve energy transfer to the lanthanide ion, the lowest triplet state energy level (T_1) of the ligand must be closely matched or slightly above the metal ion's emitting resonance levels. The suitability of the energy gap between the excited triplet energy level of the ligand and the lowest excited energy level of Ln(III) is a critical factor for sensitized luminescence of the central Ln(III) ion [56].

Three possibilities of the lowest excited resonance levels $^3P_0$ (20 300 cm^{-1}), $^1D_2$ (17 000 cm^{-1}) and $^1G_4$ (9700 cm^{-1}) of Pr(III) have taken place. However, the energy gap for $^1D_2$ level is twice as large as for the other two levels, namely $^3P_0$ and $^1G_4$. Thus, it shown that the Pr(III) ion would only emit from $^1D_2$ level due to the intramolecular energy transfer process between the oxygen atom of 18C6 ligand and Pr(III). The Pr(III) complex emits the visible and infrared luminescence in the solid state at room temperature (Fig. 7). Typical features of $^3P_0 \rightarrow ^3F_2$, $^1D_2 \rightarrow ^3F_2$ and $^1D_2 \rightarrow ^3F_4$ transitions at 650, 830 and 950 nm were observed in the Pr complex [57].

The La, Ce, Nd, Sm, Gd, Tb and Ho complexes had broad bands with the center peak at 535 nm (green) due to the 18C6 ligand and picrate anion. The picrate anion acts as quencher in the 18C6–(Ln–Pic) complexes due to the nitro withdrawing groups.

a

b
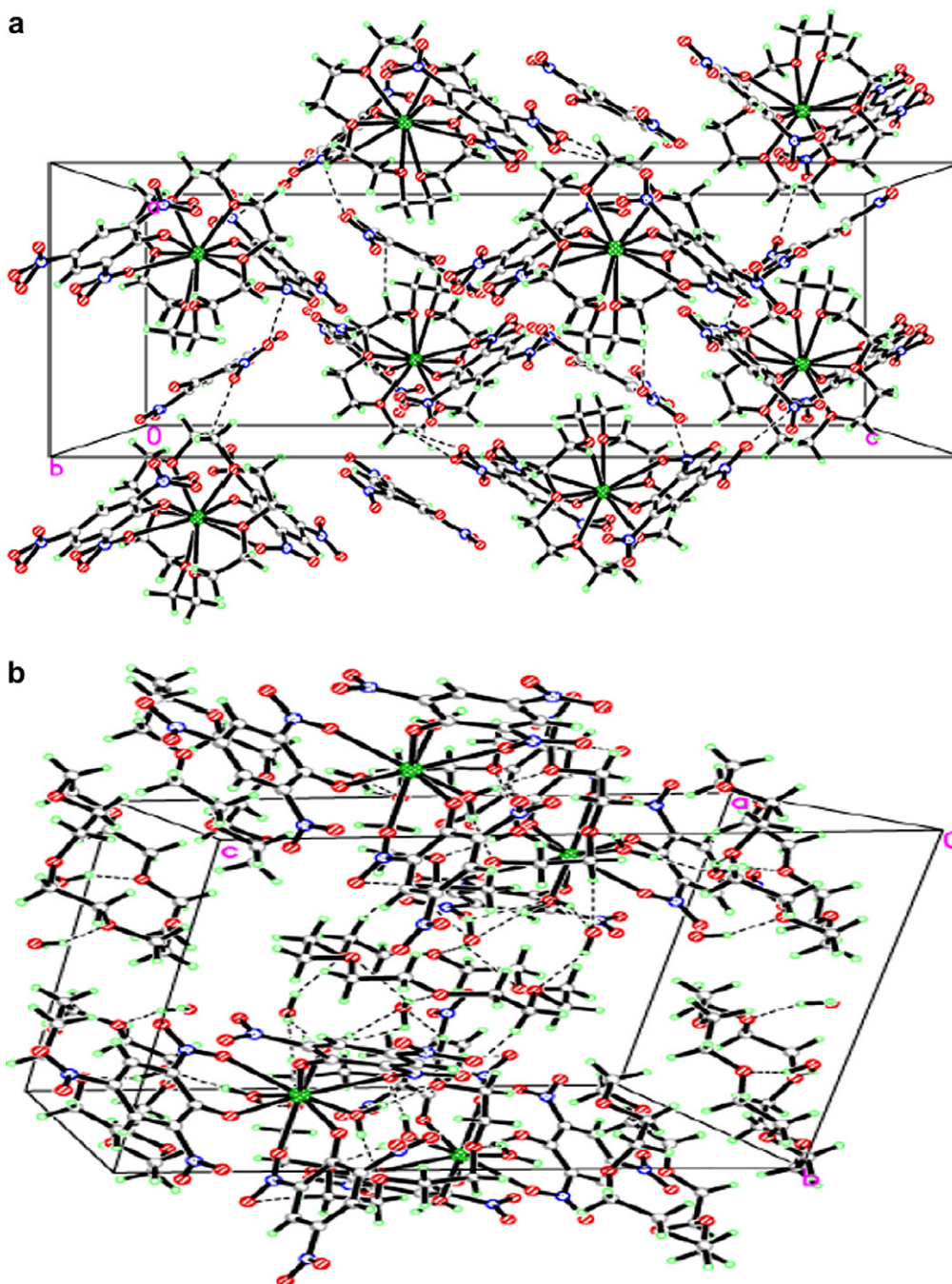
Fig. 6. Crystal packing of the La complex viewed down the *b*-axis, the dashed lines (—) show C–H···O hydrogen bonding (a) and crystal packing of the Ho complex viewed down the *a*-axis, the dashed lines (—) show O–H···O and C–H···O hydrogen bonding (b).

Near infrared (NIR) luminescence of Ln(III) ions can be quenched by O–H vibrations [58]. Due to the limitation of our equipment, we could not measure the excitation (monitored at 1540 nm) spectrum and the NIR luminescence lifetime of the Nd complex. Only the Sm, Tb and Ho complexes had a typical 4f–4f emission transitions in the visible region. For further study, only the Tb complex with the 18C6 ligand in the presence of nitrate anion was also prepared in our laboratory. The crystal structure of [Tb(NO$_3$)$_3$-(OH$_2$)$_3$](18C6) complex has been reported by Roger and Rollins [59], nevertheless the luminescence property of the this complex was not observed. Thus, we studied luminescence property of the [Tb(NO$_3$)$_3$(OH$_2$)$_3$](18C6) complex compared with the 18C6–(Tb–Pic) complex.

A strong characteristic emissions of Tb(III) for the [Tb(NO$_3$)$_3$(OH$_2$)$_3$](18C6) complex was observed. This may be due to the following factors, i.e. (i) the symmetry alteration of Tb(III) in the [Tb(NO$_3$)$_3$(OH$_2$)$_3$](18C6) complex, (ii) the good rigid structure of the complex was formed by three nitrate anions and three water molecules surrounding of the Tb(III) ion and (iii) the equivalent distances between the central Tb(III) ion and the oxygen donor atoms ranged from 2.371 to 2.446 Å. The [Tb(NO$_3$)$_3$(OH$_2$)$_3$]-(18C6) complex has a typical features of the $^5D_4 \rightarrow {}^7F_J$ ($J = 0, 1, 2, 3, 4, 5, 6$) luminescence transitions that is similar with its salt and oxide (Fig. 8). The presence of the 18C6 molecule in the complex that acts as solvated or hexadentate coordinated ligand in the inner coordination sphere influenced the luminescent peaks. The

Table 5
Hydrogen bonding in the $[Ho(Pic)_3(OH_2)_3] \cdot 2(18C6) \cdot 4(H_2O)$ complex

D–H···A	D–H (Å)	H···A (Å)	D···A (Å)	D–H···A (°)
O1W–H11W···O7W	0.860(4)	1.850(4)	2.693(2)	167.0(5)
O2W–H12W···O28	0.850	1.985	2.744(2)	148.1
O3W–H13W···O30	0.849	1.873	2.722(2)	178.2
O4W–H14W···O25	0.850	2.080	2.867(4)	153.7
O5W–H15W···O33[i]	0.851	2.167	2.923(4)	147.9
O6W–H16W···O27	0.851	2.062	2.803(5)	145.1
O7W–H17W···O1W	0.850	2.319	2.693(2)	107.0
O1W–H21W···O5W	0.840(3)	1.810(3)	2.609(4)	157.0(4)
O2W–H22W···O6W	0.850	1.841	2.689(3)	174.7
O3W–H23W···O29[ii]	0.849	1.928	2.753(2)	163.3
O5W–H25W···O1W	0.850	1.900	2.609(4)	140.1
O6W–H26W···O24	0.851	2.000	2.824(3)	162.4
O7W–H27W···O31[i]	0.850	2.006	2.832(4)	163.6
O7W–H27W···O32[i]	0.850	2.494	2.968(3)	116.1
C23–H23B···O22[a]	0.970	2.589	3.206(3)	121.6
C26–H26B···O17[iii]	0.970	2.530	3.435(4)	155.2
C32–H32A···O13[iii]	0.970	2.532	3.278(4)	133.6
C32–H32B···O5W	0.970	2.573	3.541(4)	175.0
C35–H35A···O7W	0.970	2.439	3.257(3)	141.9
C35–H35B···O10[ii]	0.970	2.475	3.418(4)	164.1
C37–H37A···O20[i]	0.960	2.465	3.255(5)	139.5
C40–H40B···O5[iv]	0.969	2.510	3.431(4)	158.6

Symmetry codes: (i) $1 - x, 1 - y, 1 - z$; (ii) $1 - x, -y, 1 - z$; (iii) $-1 + x, y, z$; (iv) $-1 + x, y, 1 + z$.
[a] Intramolecular hydrogen bonding.
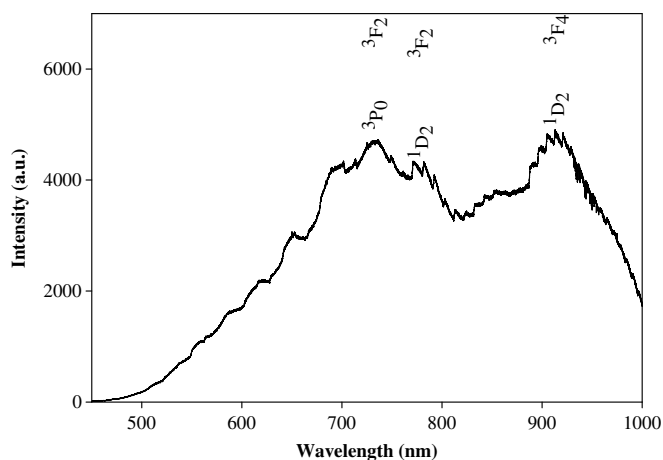
Fig. 7. The photoluminescence of the Pr complex in the solid state at room temperature.
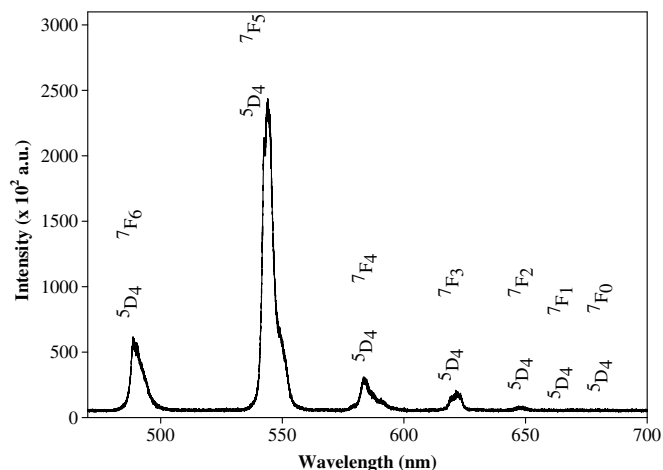
Fig. 8. The photoluminescence of the $[Tb(NO_3)_3(OH_2)_3](18C6)$ complex in the solid state at room temperature.

hypersensitive peak of the $^5D_4 \rightarrow {}^7F_5$ transition for the $[Tb(NO_3)_3(OH_2)_3](18C6)$ complex [544.2 nm; 2439×10^2 a.u.] is higher than that was found in $Tb(NO_3)_3 \cdot 6H_2O$ [541.4 nm; 298.7×10^2 a.u.] and Tb_4O_7 [542.1 nm; 41.1×10^2 a.u.]. Additionally, the purity of green emission from the $[Tb(NO_3)_3(OH_2)_3](18C6)$ complex is higher than that was found in its salt and oxide.

4. Conclusion

The rigid 18C6 ligand governs the selectivity in the formation of the complexes with Ln(III) ions in the presence of picrate anion. The Ln–O bond length is greatly influenced by the size of the Ln(III) ionic radius of due to lanthanide contraction. The contraction of the radii of the metal ions necessitates a change in the coordination environment. Different coordination environments and species in the lattice result in different non-covalent interactions which finally generate different supramolecular architectures. The picrate anion has a high steric effect to control in the inner coordination sphere of the complexes. The photoluminescence spectrum of the Pr complex has 4f–4f emission, i.e. $^3P_0 \rightarrow {}^3F_2$, $^1D_2 \rightarrow {}^3F_2$ and $^1D_2 \rightarrow {}^3F_4$ transitions.

Acknowledgements

Appendix A. Supplementary material

CCDC 237057, 667007, 667008, 667009, 667010, 667011, 667012 contains the supplementary crystallographic data for Nd, La, Ce, Gd, Ho. These data can be obtained free of charge from The Cambridge Crystallographic Data Centre via www.ccdc.cam.ac.uk/data_request/cif.

References

[1] P.J. Hagman, D. Hagan, J. Zubieta, Angew. Chem., Int. Ed. Engl. 38 (1999) 2638.
[2] B. Moulton, M.J. Zaworotko, Chem. Rev. 101 (2001) 1629.
[3] M. O'Keeffe, M. Eddaoudi, H. Li, T. Reineke, O.M. Yaghi, J. Solid State Chem. 152 (2000) 3.
[4] V.V. Ponomarova, K.V. Domasevitch, Crystal. Eng. 5 (2002) 137.
[5] R. Centore, A. Tuzi, Crystal. Eng. 6 (2003) 87.
[6] G.R. Desiraju, Angew. Chem., Int. Ed. Engl. 34 (1995) 2311.
[7] P.K. Thalapally, G.R. Desiraju, M. Bagieu-Beucher, R. Masse, C. Bourgogne, J.F. Nicoud, Chem. Commun. (2002) 1052.
[8] J. Ramkumar, Spectrochim. Acta, Part A 65 (2006) 993.
[9] J. Gao, G. Zhao, J. Kang, Talanta 42 (1995) 1497.
[10] R.C. Evans, P. Douglas, C.J. Winscom, Coord. Chem. Rev. 250 (2006) 2093.
[11] J. Li, L. Zhang, L. Liu, G. Liu, D. Jia, G. Xu, Inorg. Chim. Acta 360 (2007) 1995.
[12] S.A. Cotton, in: R.B. King (Ed.), Encyclopedia of Inorganic Chemistry, 7, Wiley, New York, 1994, p. 3595.
[13] S.A. Cotton, Coord. Chem. Rev. 160 (1997) 93.
[14] S. Isiguro, Y. Umebayashi, K. Komiya, Coord. Chem. Rev. 226 (2002) 103.
[15] L. Helm, A.E. Merbach, Coord. Chem. Rev. 187 (1999) 151.
[16] S. Zhang, K. Wu, A.D. Sherry, J. Am. Chem. Soc. 124 (2002) 4226.
[17] J.-C.G. Bünzli, N. Andre', M. Elhabiri, G. Muller, C. Piguet, J. Alloy. Compd. 303–304 (2000) 66.
[18] G. Malandrino, I.L. Fragalà, Coord. Chem. Rev. 250 (2006) 1605.
[19] P.L. Jones, A.J. Amoroso, J.C. Jeffery, J.A. McCleverty, E. Psillakis, L.H. Rees, M.D. Ward, Inorg. Chem. 36 (1997) 10.
[20] D. Xue, S. Zuo, H. Ratajczak, Physica B 352 (2004) 99.
[21] Z.X. Zhou, W.C. Zheng, Y.Z. Li, Z.H. Mao, Z.H. Zhou, Z. Hong, Polyhedron 15 (1996) 3519.
[22] D. Wang, X. Sun, H. Hu, Y. Liu, B. Chen, Z. Zhou, K. Yu, Polyhedron 8 (1989) 2051.
[23] Z. Zhou, Y. Zhou, Y. Li, K. Ding, Polyhedron 14 (1995) 3033.
[24] J.W. Steed, Coord. Chem. Rev 215 (2001) 171.
[25] A.V. Bajaj, N.S. Poonia, Coord. Chem. Rev 87 (1988) 55.
[26] F.R. Fronczek, R.D. Gandour, in: Y. Inone, G.W. Goke (Eds.), Cation Binding by Macrocycles: Complexation of Cationic Species by Crown Ethers, M. Dekker Inc., New York, 1990.

[27] R.M. Izatt, J.S. Bradshaw, S.A. Nielson, J.D. Lamb, J.J. Christensen, Chem. Rev. 85 (1985) 271.
[28] A.Y. Tsivadze, A.A. Varnek, V.E. Khutorsky, Coordination Compounds of Metals with Crown Ligands, Nauka, Moscow, 1991.
[29] I.A. Kahva, D. Miller, M. Mitchel, F. Fronczek, R.G. Goodrich, D.J. Willias, C.A. O'Mahoney, A.M. Slawin, S.V. Ley, C.G. Groombridge, Inorg. Chem. 31 (1992) 3963.
[30] R.D. Rogers, M.M. Benning, Acta Crystallogr., Sect. C 44 (1988) 1397.
[31] M.I. Saleh, A. Salhin, B. Saad, Analyst 120 (1995) 2861.
[32] J.M. Harrowfield, W. Lu, B.W. Skelton, A.H. White, Aust. J. Chem. 47 (1994) 321.
[33] M.I. Saleh, E. Kusrini, B. Saad, R. Adnan, A.S. Mohamed, B.M. Yamin, J. Lumin. 126 (2007) 871.
[34] Bruker, SADABS (Version 2.01), SMART (V5.603) and SAINT (V 6.36a). Bruker AXS Inc., Madison, Wisconsin, USA, 2000.
[35] G.M. Sheldrick, SHELXTL V5.1. Bruker AXS Inc., Madison, Wisconsin, USA, 1997.
[36] A.L. Spek, J. Appl. Crystallogr. 36 (2003) 7.
[37] W.J. Geary, Coord. Chem. Rev. 7 (1971) 81.
[38] N. Yang, J. Zheng, W. Liu, N. Tang, K. Yu, J. Mol. Struct. 657 (2003) 180.
[39] M.I. Saleh, E. Kusrini, R. Adnan, I.A. Rahman, B. Saad, A. Usman, H.-K. Fun, B.M. Yamin, J. Chem. Crystallogr. 35 (2005) 469.
[40] M.I. Saleh, E. Kusrini, R. Adnan, B. Saad, B.M. Yamin, H.K. Fun, J. Mol. Struct. 837 (2007) 169.
[41] Y. Tang, D.-B. Liu, W.-S. Liu, M.-Y. Tan, Spectrochim. Acta, Part A 63 (2006) 164.
[42] L. Fan, W. Liu, X. Gan, N. Tang, M. Tan, W. Jiang, K. Yu, Polyhedron 19 (2000) 779.
[43] P. Miranda Jr., J. Zukerman-Schpector, P.C. Isolani, G. Vicentini, L.B. Zinner, J. Alloy. Compd. 323–324 (2001) 14.
[44] N.F. Curties, Y.M. Curties, Inorg. Chem. 4 (1965) 801.
[45] L.F. Delboni, G.O. Livia, E.E. Castellano, L.B. Zinner, S. Braun, Inorg. Chim. Acta 221 (1994) 169.
[46] A.G. Silva, G. Vicentini, J. Zukerman-Schpector, E.E. Castellano, J. Alloy. Compd. 225 (1995) 354.
[47] T. Yongchi, L. Yingqiu, N. Jiazan, J. Mol. Sci. 5 (1987) 83.
[48] K. Nakagawa, K. Amita, H. Mizuno, Y. Inoue, T. Hakushi, Bull. Chem. Soc. Jpn. 60 (1987) 2037.
[49] J.C. Fernandes, J. R Matos, L. B Zinner, G. Vicentini, J. Zukerman-Schpector, Polyhedron 19 (2000) 2315.
[50] R.D. Shannon, Acta Crystallogr. A 32 (1976) 751.
[51] R.D. Rogers, A.N. Rollins, R.D. Etzenhouser, E.J. Voss, C.B. Bauer, Inorg. Chem. 32 (1993) 3451.
[52] R.D. Rogers, A.N. Rollines, R.F. Henry, J.S. Murdoch, R.D. Etzenhouser, S.E. Huggins, L. Nunez, Inorg. Chem. 30 (1991) 4946.
[53] R.D. Rogers, L.K. Kurihara, Inorg. Chem. 26 (1987) 1498.
[54] R.D. Rogers, A.N. Rollins, Inorg. Chim. Acta 230 (1995) 177.
[55] R.D. Rogers, C.B. Bauer, in: J.L. Atwood (Ed.), Comprehensive Supramolecular Chemistry, vol. 1, Pergamon Express, United State American, 1996, pp. 315–355.
[56] Y.S. Yang, M.L. Gong, Y.Y. Li, H.Y. Lei, S.L. Wu, J. Alloy. Compd. 207–208 (1994) 112.
[57] A.I. Voloshin, N.M. Shavaleev, V.P. Kazakov, J. Lumin. 93 (2001) 199.
[58] A. Beeby, I.M. Clarkson, R.S. Dickins, S.F. Aulkner, D. Parker, L. Royle, A.S. de Sousa, J.A.G. Williams, M. Woods, J. Chem. Soc., Perkin Trans. 2 (1999) 493.
[59] R.D. Rogers, A.N. Rollins, J. Chem. Crystallogr. 24 (1994) 321.